Blue Electrofluorescence Properties of Furan–Silole Ladder Pi-Conjugated Systems

Hui Chen, Mathieu Denis, Pierre-Antoine Bouit, Yinlong Zhang, Xinda Wei, Denis Tondelier, Bernard Geffroy, Zheng Duan, Muriel Hissler

applied sciences

MDPI

Article

Blue Electrofluorescence Properties of Furan–Silole Ladder Pi-Conjugated Systems

Hui Chen [1,5], Mathieu Denis [2], Pierre-Antoine Bouit [2], Yinlong Zhang [1], Xinda Wei [1], Denis Tondelier [3], Bernard Geffroy [4], Zheng Duan [1,*] and Muriel Hissler [2,*]

1 College of Chemistry and Molecular Engineering, International Phosphorus Laboratory, International Joint Research Laboratory for Functional Organophosphorus Materials of Henan Province, Zhengzhou University, Zhengzhou 450001, China; 13783466648@163.com (H.C.); 18236992693@163.com (Y.Z.); weixinda717@163.com (X.W.)

2 Université Rennes, CNRS, ISCR-UMR 6226, F-35000 Rennes, France; M.Denis@soton.ac.uk (M.D.); pierre-antoine.bouit@univ-rennes1.fr (P.-A.B.)

3 LPICM, CNRS, Ecole Polytechnique, Université Paris Saclay, 91128 Palaiseau, France; denis.tondelier@polytechnique.edu

4 LICSEN, NIMBE, CEA, CNRS, Université Paris-Saclay, CEA Saclay, Gif-sur-Yvette CEDEX 91191, France; bernard.geffroy@polytechnique.edu

5 Institute of Chemistry Henan Academy of Sciences, Zhengzhou 450002, China

* Correspondence: duanzheng@zzu.edu.cn (Z.D.); muriel.hissler@univ-rennes1.fr (M.H.); Tel.: +86-371-6778-3391 (Z.D.); +33-223235783 (M.H.)

Received: 14 April 2018; Accepted: 9 May 2018; Published: 18 May 2018

Abstract: A synthetic route to novel benzofuran fused silole derivatives is described and the new compounds were fully characterized. These compounds showed optical and electrochemical properties that differ from their benzothiophene analog. Preliminary results show that these derivatives can be used as blue emitters in organic light emitting devices (OLEDs) illustrating the potential of these new compounds for opto-electronic applications.

Keywords: π-conjugated systems; heterocycles; fluorescence; OLED

1. Introduction

Synthesis of heteroatomic π-conjugated systems for opto-electronic applications is a highly developed research field since two decades [1]. Following the successful incorporation of thiophene oligomers and polymers in opto-electronic devices, [1–3] new derivatives featuring B [4,5], N [6,7], O [8,9], Si [10] or P [11–19] have been developed. In particular, siloles (silacyclopentadienes) found promising applications in the field of organic light emitting devices (OLEDs) [20–23]. Two main reasons explain the good behaviour of siloles in these devices. First of all, the σ*-π* hyperconjugation between the exocyclic Si-C bonds and the π* orbital of the butadiene moiety drastically lower the LUMO of the siloles, thus enhancing its electron transport ability [10]. Furthermore, the presence of phenyl (or (hetero)-aryl) substituents in the 2,3,4,5 positions of the silole ring (derivative **A**, Figure 1) make it a very efficient solid-state emitter due to the so-called Aggregation-Induced Emission (AIE) effect [24–27]. This particular effect is attributed to the restriction of intramolecular rotation of the lateral phenyl rings in the aggregated state. The combination of good charge transport properties as well as high photoluminescence quantum yields in the solid state explain the good performances of the devices. Furthermore, following the pioneering work of Tamao, Yamaguchi et al., new synthetic pathways have been developed to prepare silole-containing polyacenes **B** (Figure 1), namely Si-containing ladder-π-conjugated systems [28–36]. Others families of fused silole derivatives such as Si-containing helicenes [37,38] and small 2D Polycyclic Aromatic Hydrocarbons (PAHs) [39] were

also recently prepared. Other than the synthetic challenge of preparing these derivatives, they appeared highly emissive in solution. However, poor solid-state emission was reported due to strong packing and thus no electroluminescent devices based on these structures have been prepared. However, planar molecules can be used as emitters in OLEDs if an efficient control of the packing of these planar structures in solid state is achieved, allowing to restore their emissive properties. For example, we recently reported on the preparation of ladder-benzofuran fused phospholes **C** (Figure 1) showing efficient electroluminescent properties in OLEDs if the compound **C** is diluted in a 4,4′-bis(2,2-diphenylvinyl)-1,1′-biphenyl (DPVBi) matrix [40]. Since Si-containing planar-π-conjugated systems (Figure 1B) and benzofuran fused-π-conjugated systems (Figure 1C) are highly efficient emitters, we decided to develop and study the properties of Si,O-ladder π-conjugated systems (Scheme 1) as potential efficient fluorescent emitters in OLEDs.

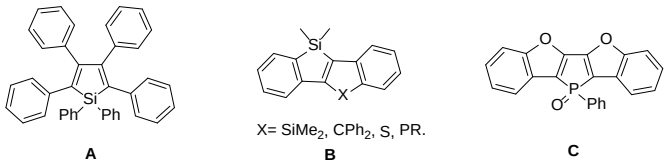

Figure 1. Reported 2,3,4,5 subsituted siloles, ladder Si,X derivatives and P,O ladder derivative.

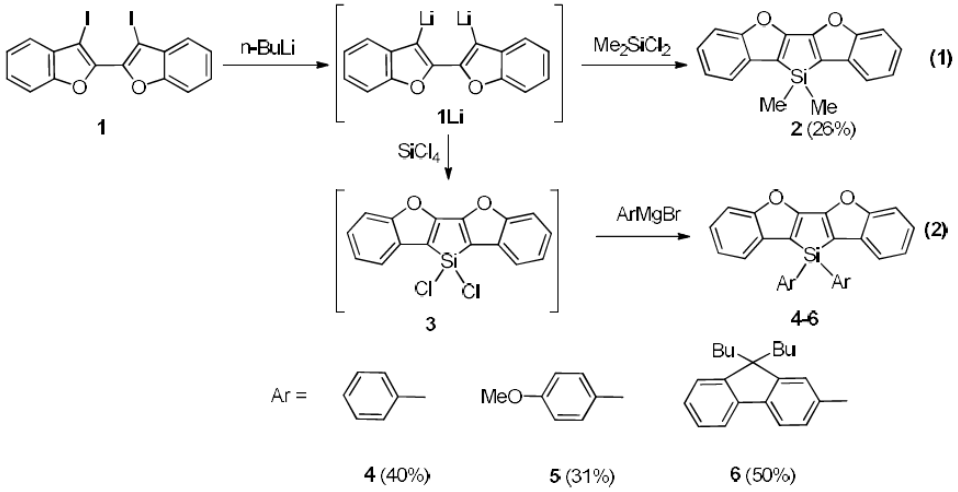

Scheme 1. Synthetic route toward **2–6.**

In the present article, we report on the use of blue-emitting Si,O-ladder π-conjugated systems as emitters in OLEDs showing that these systems can find applications in electroluminescent devices. Furthermore, we detail their synthesis and electronic properties determined experimentally (UV-vis, fluorescence, electrochemistry) and theoretically (density functional theory (DFT)).

2. Materials and Methods

All experiments were performed in an atmosphere of dry argon using standard Schlenk techniques. Commercially available reagents were used as received without further purification. Separations were performed by gravity column chromatography on silica gel (Merck Geduran 60, 0.063–0.200 mm). ^{1}H, ^{13}C and ^{29}Si spectra were recorded on a on Bruker AV III 300 (Bruker, Billerica, MA, USA) and 400 MHz NMR (Nuclear Magnetic Resonance) spectrometers. ^{1}H and ^{13}C NMR chemical shifts were reported in parts per million (ppm) relative to Me_4Si as external standard. High-resolution mass spectra were obtained on a Varian MAT 311 or ZabSpec TOF Micromass instrument (Varian, Palo Alto, CA, USA) at Scanmat, University of Rennes 1. Elemental analyses were performed by Scanmat, University of Rennes 1. Iodo-substituted benzofuran **1** was synthesized according to the

published procedure [32,41]. UV-Visible spectra were recorded at room temperature on a VARIAN Cary 5000 spectrophotometer (Varian, Palo Alto, CA, USA). The UV-Vis-NIR emission and excitation spectra measurements were recorded on a FL 920 Edimburgh Instrument (Edimburgh, Livingston, UK) equipped with a Hamamatsu R5509-73 photomultiplier (Hamamatsu, Japan) for the NIR domain (300–1700 nm) and corrected for the response of the photomultiplier. Quantum yields were calculated relative to quinine sulfate (ϕ = 0.54 in H_2SO_4 0.1 M). The electrochemical studies were carried out under argon using an Eco Chemie Autolab PGSTAT 30(Metrohm, Herisau, Switzerland) potentiostat for cyclic voltammetry with the three-electrode configuration: the working electrode was a platinum disk, the reference electrode was a saturated calomel electrode and the counter-electrode a platinum wire. All potentials were internally referenced to the ferrocene/ferrocenium couple. For the measurements, concentrations of 10^{-3} M of the electroactive species were used in freshly distilled and degassed dichloromethane or tetrahydrofuran and 0.2 M tetrabutylammonium hexafluorophosphate.

2.1. Synthesis and Characterization

2: *n*-BuLi (1.25 mL, 2.0 mmol) was added dropwise to a solution of **1** (490 mg, 1.0 mmol) in THF (20 mL) at −110 °C. After stirring for 10 min, Me_2SiCl_2 (134 µL, 1.1 mmol) was added at −78 °C and the resulting suspension was allowed to warm quickly to room temperature and stirred overnight at room temperature. After evaporation of the solvent, **2** was purified by column chromatography on silica (petroleum ether) and recrystallized from hexane to give white crystals (75 mg, 0.26 mmol, 26% yield). ^{1}H NMR (300 MHz, $CDCl_3$): δ = 0.60 (s, 6H, CH_3), 7.22–7.29 (m, 4H, Ar-H), 7.51–7.60 (m, 4H, Ar-H); ^{13}C NMR (75 MHz, $CDCl_3$): δ = −3.5 (CH_3), 112.1 (CH), 117.4 (C_{quat}), 121.5 (CH), 123.8 (CH), 124.0 (CH), 130.6 (C_{quat}), 158.5 (C_{quat}), 159.0 (C_{quat}). ^{29}Si NMR (80 MHz, $CDCl_3$): δ = −12.5 (s). HRMS Calcd for $C_{18}H_{14}O_2Si(M^+)$: 290.0763; Found: 290.0760. Anal. Calcd. for $C_{18}H_{14}O_2Si$ (C, 74.45, H, 4.86); Found: C, 74.43, H, 4.70.

3: *n*-BuLi (1.25 mL, 2.0 mmol) was added dropwise to a solution of **1** (490 mg, 1.0 mmol) in THF (20 ml) at −110 °C. After stirring for 10 min, the resulting solution was cannulated into a solution of $SiCl_4$ (460 µL, 4 mmol) in THF (10 mL) at −78 °C. The reaction mixture was stirred at room temperature overnight. Then the solvents were removed by vacuum, and the resultant reactive intermediate **3** was used in situ for the synthesis of siloles **4**–**6** without isolation.

4: To a 25 mL flask was added 5 mL Et_2O, magnesium shavings (72 mg, 3 mmol), bromobenzene (324 µL, 3 mmol), iodine and the mixture was stirred at 40 °C for 2 h. The gray suspension was slowly transferred into a THF solution of **3** at −78 °C. The brown mixture was gradually warmed to room temperature, and stirred overnight. The solvent was removed, and the residue was purified by column chromatography on silica (hexane/DCM = 5/1) and recrystallized from hexane and DCM to afford white crystals (165 mg, 0.4 mmol, 40% yield). ^{1}H NMR (300 MHz, $CDCl_3$): δ = 7.28–7.44 (m, 10H), 7.60–7.68 (m, 4H), 7.76–7.77 (m, 4H); ^{13}C NMR (75 MHz, $CDCl_3$): δ = 112.3 (CH), 115.3 (C_{quat}), 121.7 (CH), 124.2 (CH), 124.4 (CH), 128.5 (CH), 130.5 (C_{quat}), 130.7 (CH), 130.8 (C_{quat}), 135.3 (CH), 158.7 (C_{quat}), 159.9 (C_{quat}). ^{29}Si NMR (80 MHz, $CDCl_3$): δ = −21.6 (s). HRMS Calcd for $C_{28}H_{18}O_2Si(M^+)$: 414.1076; Found: 414.1074. Anal. Calcd. for $C_{28}H_{18}O_2Si$ (C, 81.13, H, 4.38); Found: C, 81.49, H, 4.17.

5: To a 25 mL flask was added 5 mL Et_2O, magnesium shavings (72 mg, 3 mmol), 4-bromoanisole (375 µL, 3 mmol), iodine, and the mixture was stirred at 40 °C for 2 h. The gray suspension was slowly transferred portion wisely into the THF solution of **3** at −78 °C. The brown mixture was gradually warmed to room temperature, and stirred overnight. The solvent was removed, and the residue was purified by column chromatography on silica (hexane/DCM = 5/1) and recrystallized from hexane and DCM to afford white crystals (147 mg, 0.31 mmol, 31% yield). ^{1}H NMR (300 MHz, $CDCl_3$): δ = 3.78 (s, 6H, OMe), 6.92 (d, ^{3}J(H,H) = 7 Hz, 4H), 7.27–7.30 (m, 4H), 7.59–7.64 (m, 4H), 7.66 (d, ^{3}J(H,H) = 7 Hz, 4H); ^{13}C NMR (75 MHz, $CDCl_3$): δ = 55.1 (OCH_3), 112.2 (CH), 114.3 (CH), 115.9 (C_{quat}), 121.6 (C_{quat}), 121.7 (CH), 124.1 (CH), 124.2 (CH), 130.6 (C_{quat}), 136.9 (CH), 158.7 (C_{quat}), 159.7 (C_{quat}), 161.7 (C_{quat}). ^{29}Si NMR (80 MHz, $CDCl_3$): δ = −22.2 (s). HRMS Calcd for $C_{30}H_{22}O_4Si(M^+)$: 474.1287; Found: 474.1286. Anal. Calcd. for $C_{30}H_{22}O_4Si$ (C, 75.92, H, 4.67); Found: C, 75.60, H, 4.39.

6: To a 25 mL flask was added 5 mL THF, magnesium shavings (72 mg, 3 mmol), 2-bromo-9,9-dibutyl-fluorene (1068 mg, 3 mmol), iodine, and the mixture was refluxed for 3 h. The gray Grignard reagent suspension was slowly transferred portion wise into the THF solution of **3** at −78 °C. The brown mixture was gradually warmed to room temperature, and stirred overnight. The solvent was removed, and the residue was purified by column chromatography on silica (hexane/DCM = 5/1) and recrystallized from hexane and DCM to afford white crystals (408 mg, 0.5 mmol, 50% yield). ^{1}H NMR (300 MHz, $CDCl_3$): δ = 0.54–0.63 (20H), 0.97–1.05 (8H, CH_2), 1.87–1.93 (8H, CH_2), 7.28–7.33 (m, 10H), 7.62–7.74 (m, 10H), 7.78 (s, 2H); ^{13}C NMR (75 MHz, $CDCl_3$): δ = 13.8 (CH_3), 23.0 (CH_2), 26.0 (CH_2), 39.8 (CH_2), 55.0 (C_{quat}), 112.2 (CH), 116.1 (C_{quat}), 119.8 (CH), 120.1 (CH), 121.5 (CH), 123.0 (CH) 124.1 (CH), 124.2 (CH), 126.8 (CH), 127.7 (CH), 129.0 (C_{quat}), 129.8 (CH), 130.7 (C_{quat}), 134.0 (CH), 140.5 (C_{quat}), 143.7 (C_{quat}), 150.5 (C_{quat}), 151.0 (C_{quat}), 158.7 (C_{quat}), 160.0 (C_{quat}). ^{29}Si NMR (80 MHz, $CDCl_3$): δ = −21.3 (s). HRMS Calcd for $C_{30}H_{22}O_4Si(M^+)$: 814.4206; Found: 814.4196. Anal. Calcd. for $C_{58}H_{58}O_2Si$ (C, 85.46, H, 7.17); Found: C, 84.96, H, 7.00.

2.2. Device Fabrication and Characterization

Electroluminescent (EL) devices, based on a multilayer structure have been fabricated onto patterned ITO coated glass substrates from Xin Yang Technology (90 nm thick and sheet resistance below 20 Ω/sq). Prior to organic layer deposition, the ITO substrates were carefully cleaned. The organic materials (from Aldrich and Syntec) are deposited onto the ITO anode by sublimation under high vacuum (<10^{-6} Torr) at a rate of 0.2–0.3 nm/s. The common structure of all the devices (**A**–**G**) is the following: 10 nm of CuPc/40 nm of α-NPB/ 10 nm of TcTa/ 20 nm of emitting layer/50 nm of TPBi/1.2 nm of LiF and 100 nm of aluminum as the cathode. The copper phtalocyanine (CuPc) is used as the hole injection layer (HIL), *N*,*N*′-diphenyl-*N*,*N*′-bis(1-naphthylphenyl)-1,1′-biphenyl-4,4′-diamine (α-NPB) and Tris(4-carbazoyl-9-ylphenyl)amine (TcTa) as hole transporting layers (HTL) and 1,3,5-tris(*N*-phenylbenzimiazole-2-yl)benzene (TPBi) as the electron transport layer (ETL). The emitting layer is the pure compound (devices A and D) or a guest/host system (devices B, C and E–G) with the compound used as a dopant in 1,3-Bis(*N*-carbazolyl)benzene (mCP) matrix. The guest/host layer is obtained by co-evaporation of the two materials and the doping rate is controlled by tuning the evaporation rate of each material. In this study, the thicknesses of the different organic layers were kept constant for all the devices. The active area of the devices defined by the overlap between the ITO anode and the metallic cathode was 0.3 cm^2. The current-voltage-luminance (I-V-L) characteristics of the devices were measured with a regulated power supply (Laboratory Power Supply EA-PS 3032-10B) combined with a multimeter and a 1 cm^2 area silicon calibrated photodiode (Hamamatsu). The spectral emission was recorded with a SpectraScan PR650 spectrophotometer (Photo research, North Syracuse, NY, USA). All the measurements were performed at room temperature and at ambient atmosphere, with no further encapsulation of devices.

3. Results and Discussion

The most straightforward synthetic route to furan–silole ladder compounds may be the reaction of the dimetalated dibenzofuran with R_2SiCl_2 (Scheme 1), a similar procedure was reported for the synthesis of dibenzofuran-fused phosphole [40]. Effectively, the treatment of iodo-substituted benzofuran **1** with two equivalents of *n*BuLi produces the corresponding dianion, which was then quenched with Me_2SiCl_2 at −78 °C leading to compound **2** in moderate yield (26%). This compound was fully characterized by NMR spectroscopies. In particular, a singlet at about δ = +0.60 ppm in ^{1}H NMR spectrum and a ^{13}C NMR signal at −3.55 ppm confirmed the presence of Si-CH_3 bond. High Resolution Mass Spectrometry and elemental analysis also confirmed the proposed structure. However, under similar conditions, the reaction with Ph_2SiCl_2 provided only negligible amount of compound **4**, as already published by Ohshita et al. [14] This might be due to the low reactivity of the dilithiated intermediate **1Li**. Thus, the procedure was modified to prepare compounds **4**–**6**

from the reaction of **1Li** with highly reactive and less bulky $SiCl_4$. Dichloro-substituted silole **3** was formed in situ, then the reaction mixture was treated with two equivalents of the corresponding aryl substituted Grignard reagent. This stepwise introduction of aryl groups on the silicon atom was successful for the preparation of bisaryl-substituted siloles since compounds **4**–**6** have been isolated in good yields after column chromatography (31–50%) and were characterized by HRMS, elemental analysis, and multinuclear NMR spectroscopies. All these data are consistent with the proposed structures. Furthermore, the ^{29}Si and ^{13}C NMR shifts around the silole rings of these novel ladder furan–siloles derivatives are different from their thiophene and indole analogues [41–43], (^{29}Si NMR: δ (ppm) = −23.2 (indole based derivative [32]); −18.8 (Benzothiophene-based derivative [32]); −21.1 (**4**)) suggesting that the different aromaticity's of the O-, N- and S- fused cycles influences the electronic distribution within the fused frameworks.

The crystal packing of compound **4** was investigated by X-ray diffraction (XRD) measurements. Single crystals of **4** were obtained by slow evaporation of hexane-dichloromethane mixture solution at room temperature (Figure 2 and Table S1) The fused conjugated system featuring the five heterocycles is almost planar. However, the rather long C-Si bond (d = 1.8692(19) Å) causes a slight distortion of the backbone (Si-C_1-C_2-C_3 = 11.8(4)° for **4** for example) (see Table S2). The bond length alternation inside the silole ring are classical ($d_{C=C}$ = 1.346(3) Å; d_{C-C} = 1.445(4) Å). As observed for its P-analog, the bond lengths in the furan ring are dissymmetric (d_1 = 1.393(3) Å; d_2 = 1.346(3) Å for **4**) reflecting the aromaticity differences of the ring it is fused to (respectively phenyl and siloles). At the intermolecular level, Compound **4** crystallizes as infinite columns in which the fused benzofuran moieties of two different molecules are in π-stacking interactions (d = 3.636 Å) (see Figure 2).

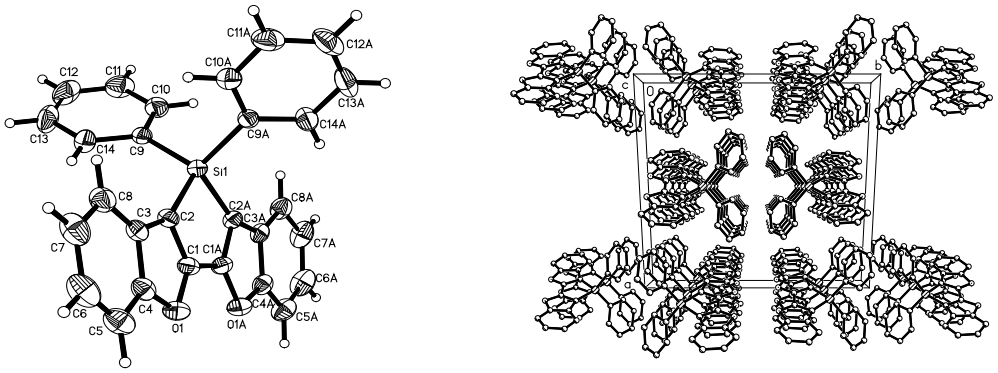

(**a**) (**b**)

Figure 2. Molecular structure of **4** (thermal ellipsoids 50% probability). (**a**) view of crystallographic structure of **4** and (**b**) view of the packing structure of **4** and the hydrogen atoms are omitted for clarity.

The optical properties (UV-vis absorption and fluorescence) of compounds **2**, **4**–**6** were studied in dichloromethane (Figure 3, and Table 1). As anticipated, the four compounds **2**, **4**–**6** show similar absorption with a broad band in the visible range ($\lambda_{max} \approx 370$ nm, Figure 3). This absorption band is attribute to a π-π* transition of the heteropentacenic backbone. Density functional theory calculations (DFT) performed on compounds **2** and **4** at the B3LYP/6-311+G (d, p) level (Figure 3 and Table S3, Figure S3) [44] show that both the HOMO (Highest Occupied Molecular Orbital) and LUMO (Lowest Occupied Molecular Orbital) are localized on the entire π-conjugated carbon framework with a contribution of σ*-π* in the LUMO. Thus, the exocyclic groups linked to the Si atom can have an influence on the optical properties. For example, compound **2**, with the methyl groups attached to the silicon atom, displays a λ_{max} blue-shifted around 10 nm compared to compounds **4**–**6** featuring aryl substituents. Note that the UV signature of the fluorenyl group is present between 270 nm and 320 nm in the case of **6**. A similar trend is observed for the fluorescence of the compounds. Compounds **2**,**3**–**6**

show intense fluorescence around 430 nm with a small blue-shift for the derivative **2** ($\Delta\lambda$ = 10 nm). Excitation spectra also confirmed the observations made for the UV-vis absorption of compounds **2**, **4–6**. (see Figure S1). The solid-state luminescence of compounds **2**, **4–6** have been recorded in thin films. The solid-state luminescence of **2** is broadened and red-shifted as an effect of intermolecular interactions (see Figure S2). However, when bulky substituents are attached to the Si-atom (**4–6**), there is a good match between solution and solid-state luminescence (Figure S2), as the exocyclic fragments prevent intermolecular interaction. This is in good agreement with data previously reported for **4** [43].

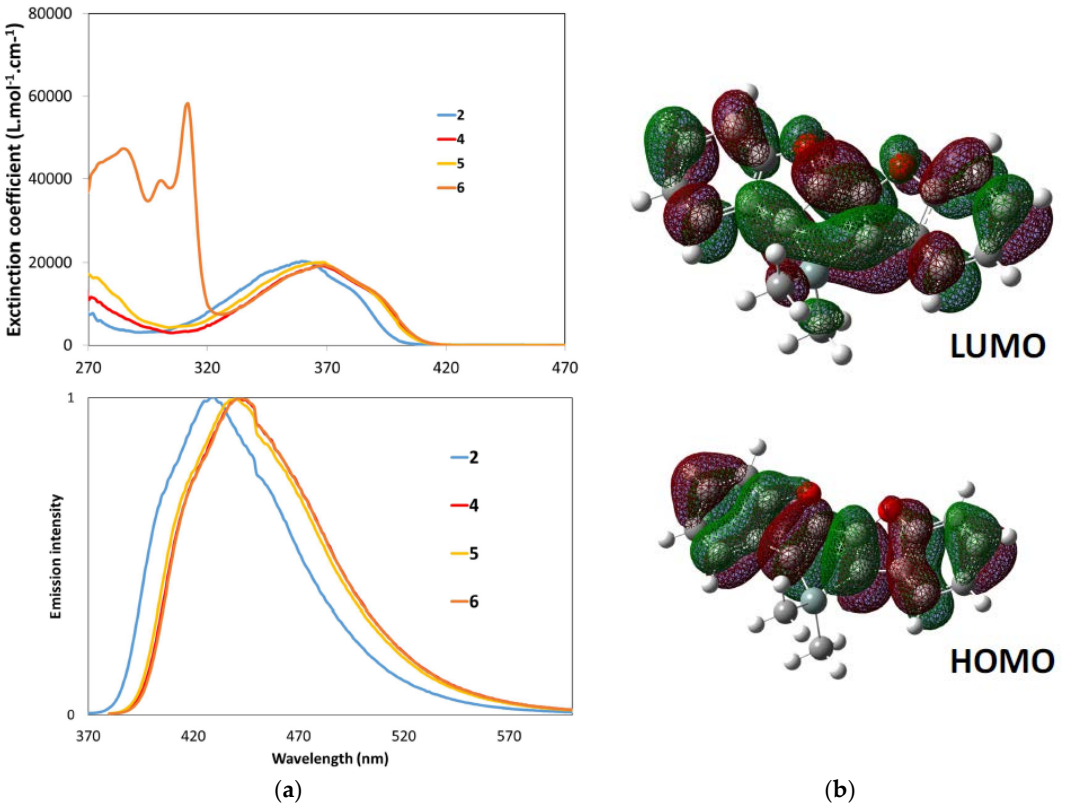

Figure 3. (**a**) UV-vis absorption (**top**) and fluorescence emission (**bottom**) of **2**, **4–6** in dichloromethane. (**b**) Calculated molecular orbitals for compound **2**.

Table 1. Photophysical and redox data.

Compound	λ_{abs} [a] [nm]	ε [L·mol^{-1}·cm^{-1}]	E_{opt} [b] eV	λ_{em} [c] [nm]	Φ_F [d]	E°_{ox} [e] [V]	E_{pc} [f] [V]	Td_{10} [g] [°C]
2	360	19,000	3.12	429	0.75	+0.72	−2.73	203
4	368	19,000	3.03	441	0.86	+0.79	−2.63	290
5	368	17,000	3.03	440	0.68	+0.78	−2.68	318
6	369	18,000	3.03	443	0.76	+0.79	−2.66	385

[a] In CH_2Cl_2 (10^{-5} M). [b] Calculated as $E_{opt} = hc/\lambda_{onset}$. [c] In CH_2Cl_2 (10^{-5} M) with (λ_{ex} = 370 nm). [d] Measured in CH_2Cl_2 relative to quinine sulfate (H_2SO_4, 1 N), ϕ_{ref} = 0.54. [e] In CH_2Cl_2 with $Bu_4N^+PF_6^-$ (0.2 M) at a scan rate of 0.1 V.s^{-1}; half-wave potential, potentials vs ferrocene/ferrocenium. [f] In THF with $Bu_4N^+PF_6^-$ (0.2 M) at a scan rate of 100 mVs^{-1}; cathodic peak (E_{pc}), potentials vs ferrocene. [g] Decomposition temperature at 10% weight loss, measured by thermogravimetric analysis (TGA) under nitrogen.

The redox properties of compounds **2**, **4–6** has been investigated by cyclic voltammetry (CH_2Cl_2 or THF, 0.2 M, $TBAPF_6$, v = 0.1 V.s^{-1}, see Table 1). All compounds show a reversible oxidation wave at relatively low potential and an irreversible reduction process at high potential. Compounds **4–6** display a mono-electronic oxidation wave at around +0.79 V (vs. Fc^+/Fc) while **2** is slightly easier to oxidize (E_{ox} = +0.72 V vs. Fc^+/Fc). Furthermore, compounds **4–6** featuring aryl substituents are

slightly easier to reduce than compound **2**. Compared to its P-congeners, compounds **2**, **4**–**6** present a higher band gap [12]. This is in line with the fact that linear phospholes oxides oligomers possess a smaller HOMO-LUMO gap compared to their Si analogs.

The thermal stability of **2**, **4**–**6** was also evaluated by means of thermogravimetric (TGA) analysis and differential scanning calorimetry (DSC) in order to evaluate if these compounds can be evaporated for the construction of OLEDs. While **2** has rather moderate thermal stability (Td_{10} = 203 °C, Table 1), the three aryl-substituted siloles **4**–**6** possess a higher stability (td_{10} > 290 °C). Notably, **6** is stable up to 385 °C, making it an appealing candidate for insertion into optoelectronic device. Interestingly, **4** and **6**, whose optical and electrochemical properties are similar, possess different thermal properties. **4** displays the classical reversible DSC curve upon cyclization (melting up on heating and crystallization upon cooling). In the case of **6**, a melting is observed during the first heating cycle, but no crystallization and further melting are observed during the next cycles. This is typical of a glassy state, probably due to the presence of 4 alkyl chains on the fluorine moiety.

Taking in account the thermal stabilities and the physical properties of compounds **2**, **4**–**6**, only compounds **4** and **6** were used as emitting material (EM) pure or doped in mCP matrix. In a first attempt, compound **4** (device **A**) and **6** (device **D**) were used as pure emitter in the device. The electroluminescence (EL) spectra are shown in Figure 4. The blue EL emission is red-shifted relative to the emission observed in diluted solution (Table 1). The red-shift is larger for compound **6** (29 nm) comparatively to compound **4** (15 nm). In these devices, luminance and external quantum efficiency (EQE) [45] are moderate (Table 2). However, the EL performance is larger for compound **4** relative to device **6**. It is believed that charge transport in **6** is low, causing this low efficiency. An increase of the performance could be observed when the compounds are used as dopant in a mCP matrix (Table 2 and Figure S2). For compound **4**, no modification of the CIE coordinates was observed when the doping ratio increases until 4.5% and an external quantum efficiency (EQE) of 2.5% and a maximum brightness of 1580 cd/m^2 can be reached. A maximum current efficiency (CE) and power efficiency (PE) of 2.8 cd/A and 1.4 Lm/W respectively are therefore obtained. Such values are quite good for the deep blue fluorescent OLED devices obtained with compound **4**. When compound **6** is used as dopant in the mCP matrix, a blue-shift of the EL spectrum is obtained relative to the pure material. However, a decrease of electroluminescent performance is observed compared to those of compound **4.** For compound **6**, the best performance can be achieved when it is used as dopant in the mCP matrix indicating that the presence of the fluorenyl group on the Si atom doesn't favor the charge mobility in the emissive layer. This assumption is supported by the fact that the gradual increase of the doping ratio (Table 2) leads to accumulation of charges, a red-shift of the emission properties and a decrease of the performance.

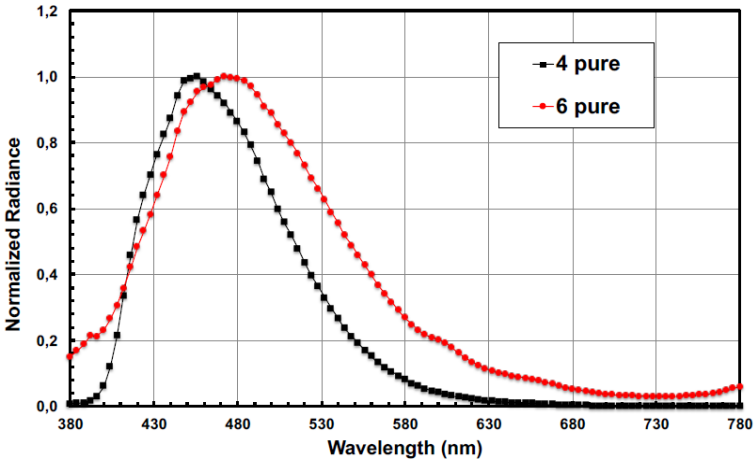

Figure 4. Normalized electroluminescence spectra of devices **A** and **D**.

Table 2. Electroluminescent performance of devices **A**–**G**.

Device	Emitter	Doping Rate (%)	Von [a] (V)	EQE [b] (%)	CE [b] (cd/A)	PE [b] (Lm/W)	CIE Color Coordinates	Maximal Brightness (cd/m^2) (@ mA/cm^2)
A	**4**	pure	3.8	1.7	2.4	1.1	0.16; 0.18	1040 (110)
B	**4**	1	3.5	2.5	2.7	1.4	0.15; 0.15	1060 (110)
C	**4**	4.5	3.5	2.4	2.8	1.4	0.15; 0.15	1580 (130)
D	**6**	pure	4.3	0.5	0.9	0.3	0.20; 0.27	270 (90)
E	**6**	1	3.9	1.3	1.3	0.6	0.18; 0.17	740 (140)
F	**6**	4	3.4	1.2	1.5	0.7	0.17; 0.19	590 (120)
G	**6**	6	3.6	1.1	1.5	0.7	0.18; 0.19	630 (150)

[a] Threshold voltage recorded at luminance of 1 cd/m^2, [b] EQE, CE and PE recorded at 10 mA/cm^2.

4. Conclusions

In conclusion, Si,O-ladder π-conjugated were synthesized and fully characterized. These derivatives display distinct optical and redox properties compared to their PO-analogs, thus emphasizing the role of the aromaticity of the heterocyclopentadiene ring in these ladder compounds. The good emission properties of **4**, together with adequate HOMO-LUMO levels and sufficient thermal stability allowed us to prepare blue emitting OLEDs, illustrating the potential of these Si-based emitters for opto-electronic applications.

Supplementary Materials: The following are available online at http://www.mdpi.com/2076-3417/8/5/812/s1.

Acknowledgments: This work was supported the National Natural Science Foundation (21672193, 21502045, 21272218, 21072179, 20702050) and Zhengzhou University. This research is supported by the Ministère de la Recherche et de l'Enseignement Supérieure, Région Bretagne, the University of Rennes 1, CNRS, China-French associated international laboratory in "Functional Organophosphorus Materials". The COST Action CM1302 (SIPS) European Network on Smart Inorganic Polymers is also acknowledged.

Conflicts of Interest: The authors declare no conflict of interest.

References

1. Roncali, J. Synthetic principles for bandgap control in linear π-conjugated systems. *Chem. Rev.* **1997**, *97*, 173–206. [CrossRef] [PubMed]
2. Mishra, A.; Ma, C.-Q.; Bauerle, P. Functional oligothiophenes: Molecular design for multidimensional nanoarchitectures and their applications. *Chem. Rev.* **2009**, *109*, 1141–1276. [CrossRef] [PubMed]
3. Hissler, M.; Dyer, P.W.; Réau, R. Linear organic π-conjugated systems featuring the heavy group 14 and 15 elements. *Coord. Chem. Rev.* **2003**, *244*, 1–44. [CrossRef]
4. Entwistle, C.D.; Marder, T.B. Boron chemistry lights the way: Optical properties of molecular and polymeric systems. *Angew. Chem. Int. Ed.* **2002**, *41*, 2927–2931. [CrossRef]
5. Dou, C.; Saito, S.; Matsuo, K.; Hisaki, I.; Yamaguchi, S. A Boron–Containing PAH as a Substructure of Boron-Doped Graphene. *Angew. Chem. Int. Ed.* **2012**, *51*, 12206–12210. [CrossRef] [PubMed]
6. Diaz, A.F.; Kanazawa, K.K.; Gardini, G.P. Electrochemical polymerization of pyrrole. *J. Chem. Soc. Chem. Commun.* **1979**, *14*, 635–636. [CrossRef]
7. Sun, M.; Wang, L.; Yang, W. Pyrrole-based narrow-band-gap copolymers for red light-emitting diodes and bulk heterojunction photovoltaic cells. *J. Appl. Polym. Sci.* **2010**, *118*, 1462–1468. [CrossRef]
8. Gidron, O.; Diskin-Posner, Y.; Bendikov, M. α-Oligofurans. *J. Am. Chem. Soc.* **2010**, *132*, 2148–2150. [CrossRef] [PubMed]
9. Woo, C.H.; Beaujuge, P.M.; Holcombe, T.W.; Lee, O.P.; Fréchet, J.M.J. Incorporation of furan into low band-gap polymers for efficient solar cells. *J. Am. Chem. Soc.* **2010**, *132*, 15547–15549. [CrossRef] [PubMed]
10. Zhan, X.; Barlow, S.; Marder, S.R. Substituent effects on the electronic structure of siloles. *Chem. Commun.* **2009**, *15*, 1948–1955. [CrossRef] [PubMed]
11. Baumgartner, T.; Réau, R. Organophosphorus π-conjugated materials. *Chem. Rev.* **2006**, *106*, 4681–4727. [CrossRef] [PubMed]

12. Bouit, P.-A.; Escande, A.; Szűcs, R.; Szieberth, D.; Lescop, C.; Nyulászi, L.; Hissler, M.; Réau, R. Dibenzophosphapentaphenes: Exploiting P chemistry for gap fine-tuning and coordination-driven assembly of planar polycyclic aromatic hydrocarbons. *J. Am. Chem. Soc.* **2012**, *134*, 6524–6527. [CrossRef] [PubMed]
13. Chen, H.; Delaunay, W.; Yu, L.; Joly, D.; Wang, Z.; Li, J.; Wang, Z.; Lescop, C.; Tondelier, D.; Geffroy, B.; et al. 2, 2′-Biphospholes: Building Blocks for Tuning the HOMO–LUMO Gap of π-Systems Using Covalent Bonding and Metal Coordination. *Angew. Chem. Int. Ed.* **2012**, *51*, 214–217. [CrossRef] [PubMed]
14. Chen, H.; Pascal, S.; Wang, Z.; Bouit, P.-A.; Wang, Z.; Zhang, Y.; Tondelier, D.; Geffroy, B.; Réau, R.; Mathey, F.; et al. 1, 2-Dihydrophosphete: A Platform for the Molecular Engineering of Electroluminescent Phosphorus Materials for Light-Emitting Devices. *Chem. Eur. J.* **2014**, *20*, 9784–9793. [CrossRef] [PubMed]
15. Ren, Y.; Kan, W.H.; Henderson, M.A.; Bomben, P.G.; Berlinguette, C.P.; Thangadurai, V.; Baumgartner, T. External-stimuli responsive photophysics and liquid crystal properties of self-assembled "phosphole-lipids". *J. Am. Chem. Soc.* **2011**, *133*, 17014–17026. [CrossRef] [PubMed]
16. Matano, Y.; Saito, A.; Fukushima, T.; Tokudome, Y.; Suzuki, F.; Sakamaki, D.; Kaji, H.; Ito, A.; Tanaka, K.; Imahori, H. Fusion of Phosphole and 1, 1′-Biacenaphthene: Phosphorus (V)-Containing Extended π-Systems with High Electron Affinity and Electron Mobility. *Angew. Chem. Int. Ed.* **2011**, *50*, 8016–8020. [CrossRef] [PubMed]
17. Joly, D.; Bouit, P.-A.; Hissler, M. Organophosphorus derivatives for electronic devices. *J. Mater. Chem. C* **2016**, *4*, 3686–3698. [CrossRef]
18. Duffy, M.P.; Delaunay, W.; Bouit, P.-A.; Hissler, M. π-Conjugated phospholes and their incorporation into devices: Components with a great deal of potential. *Chem. Soc. Rev.* **2016**, *45*, 5296–5310. [CrossRef] [PubMed]
19. Szűcs, R.; Bouit, P.-A.; Nyulászi, L.; Hissler, M. P-containing Polycyclic Aromatic Hydrocarbons. *Chem. Phys. Chem.* **2017**, *18*, 2618–2630. [CrossRef] [PubMed]
20. Tamao, K.; Uchida, M.; Izumizawa, T.; Furukawa, K.; Yamaguchi, S. Silole derivatives as efficient electron transporting materials. *J. Am. Chem. Soc.* **1996**, *118*, 11974–11975. [CrossRef]
21. Chen, H.Y.; Lam, W.Y.; Luo, J.D.; Ho, Y.L.; Tang, B.Z.; Zhu, D.B.; Wong, M.; Kwok, H.S. Highly efficient organic light-emitting diodes with a silole-based compound. *Appl. Phys. Lett.* **2002**, *81*, 574–576. [CrossRef]
22. Geramita, K.; McBee, J.; Shen, Y.; Radu, N.; Tilley, T.D. Synthesis and characterization of perfluoroaryl-substituted siloles and thiophenes: A series of electron-deficient blue light emitting materials. *Chem. Mater.* **2006**, *18*, 3261–3269. [CrossRef]
23. Lee, J.H.; Yuan, Y.Y.; Kang, Y.J.; Jia, W.L.; Lu, Z.H.; Wang, S.N. 2, 5-Functionalized Spiro-Bisiloles as Highly Efficient Yellow-Light Emitters in Electroluminescent Devices. *Adv. Funct. Mater.* **2006**, *16*, 681–686. [CrossRef]
24. Luo, J.; Xie, Z.; Lam, J.W.Y.; Cheng, L.; Chen, H.; Qiu, C.; Kwok, H.S.; Zhan, X.; Liu, Y.; Zhu, D.; et al. Aggregation-induced emission of 1-methyl-1, 2, 3, 4, 5-pentaphenylsilole. *Chem. Commun.* **2001**, 1740–1741. [CrossRef]
25. Hong, Y.; Lam, J.W.Y.; Tang, B.Z. Aggregation-induced emission: Phenomenon, mechanism and applications. *Chem. Commun.* **2009**, 4332–4353. [CrossRef] [PubMed]
26. Ding, D.; Li, K.; Liu, B.; Tang, B.Z. Bioprobes based on AIE fluorogens. *Acc. Chem. Res.* **2013**, *46*, 2441–2453. [CrossRef] [PubMed]
27. Mei, J.; Hong, Y.; Lam, J.W.Y.; Qin, A.; Tang, Y.; Tang, B.Z. Aggregation-induced emission: The whole is more brilliant than the parts. *Adv. Mater.* **2014**, *26*, 5429–5479. [CrossRef] [PubMed]
28. Yamaguchi, S.; Xu, C.; Tamao, K. Bis-silicon-bridged stilbene homologues synthesized by new intramolecular reductive double cyclization. *J. Am. Chem. Soc.* **2003**, *125*, 13662–13663. [CrossRef] [PubMed]
29. Xu, C.; Wakamiya, A.; Yamaguchi, S. Ladder Oligo(p-phenylenevinylene)s with Silicon and Carbon Bridges. *J. Am. Chem. Soc.* **2005**, *127*, 1638–1639. [CrossRef] [PubMed]
30. Mouri, K.; Wakamiya, A.; Yamada, H.; Kajiwara, T.; Yamaguchi, S. Ladder distyrylbenzenes with silicon and chalcogen bridges: Synthesis, structures, and properties. *Org. Lett.* **2006**, *9*, 93–96. [CrossRef] [PubMed]
31. Fukazawa, A.; Yamaguchi, S. Ladder π-Conjugated Materials Containing Main-Group Elements. *Chem. Asian J.* **2009**, *4*, 1386–1400. [CrossRef] [PubMed]
32. Ohshita, J.; Lee, K.-H.; Kimura, K.; Kunai, A. Synthesis of siloles condensed with benzothiophene and indole rings. *Organometallics* **2004**, *23*, 5622–5625. [CrossRef]

33. Wan, J.-H.; Fang, W.-F.; Li, Z.-F.; Xiao, X.-Q.; Xu, Z.; Deng, Y.; Zhang, L.-H.; Jiang, J.-X.; Qiu, H.-Y.; Wu, L.-B.; et al. Novel Ladder π-Conjugated Materials—Sila-Pentathienoacenes: Synthesis, Structure, and Electronic Properties. *Chem. Asian J.* **2010**, *5*, 2290–2296. [CrossRef] [PubMed]
34. Ureshino, T.; Yoshida, T.; Kuninobu, Y.; Takai, K. Rhodium-catalyzed synthesis of silafluorene derivatives via cleavage of silicon−hydrogen and carbon−hydrogen bonds. *J. Am. Chem. Soc.* **2010**, *132*, 14324–14326. [CrossRef] [PubMed]
35. Xu, Y.Z.; Wang, Z.H.; Gan, Z.J.; Xi, Q.Z.; Duan, Z.; Mathey, F. Versatile Synthesis of Phospholides from Open-Chain Precursors. Application to Annelated Pyrrole–and Silole–Phosphole Rings. *Org. Lett.* **2015**, *17*, 1732–1734. [CrossRef] [PubMed]
36. Zhou, Y.; Yang, S.; Li, J.; He, G.F.; Duan, Z.; Mathey, F. Phosphorus and silicon-bridged stilbenes: Synthesis and optoelectronic properties. *Dalton Trans.* **2016**, *45*, 18308–18312. [CrossRef] [PubMed]
37. Oyama, H.; Nakano, K.; Harada, T.; Kuroda, R.; Naito, M.; Nobusawa, K.; Nozaki, K. Facile synthetic route to highly luminescent sil [7] helicene. *Org. Lett.* **2013**, *15*, 2104–2107. [CrossRef] [PubMed]
38. Shibata, T.; Uchiyama, T.; Yoshinami, Y.; Takayasu, S.; Tsuchikama, K.; Endo, K. Highly enantioselective synthesis of silahelicenes using Ir-catalyzed [2+2+2] cycloaddition. *Chem. Commun.* **2012**, *48*, 1311–1313. [CrossRef] [PubMed]
39. Furukawa, S.; Kobayashi, J.; Kawashima, T. Development of a Sila-Friedel− Crafts Reaction and Its Application to the Synthesis of Dibenzosilole Derivatives. *J. Am. Chem. Soc.* **2009**, *131*, 14192–14193. [CrossRef] [PubMed]
40. Chen, H.; Delaunay, W.; Li, J.; Wang, Z.; Bouit, P.-A.; Tondelier, D.; Geffroy, B.; Mathey, F.; Duan, Z.; Réau, R.; et al. Benzofuran-fused phosphole: Synthesis, electronic, and electroluminescence properties. *Org. Lett.* **2013**, *15*, 330–333. [CrossRef] [PubMed]
41. Zhao, Y.; Hao, W.; Ma, W.; Zang, Z.; Zhang, H.; Liu, X.; Zou, S.; Zhang, H.; Liu, W.; Gao, J. Easily-soluble heteroacene bis (benzothieno) silole derivatives for sensing of nitro explosives. *New. J. Chem.* **2014**, *38*, 5754–5760. [CrossRef]
42. Mehta, S.; Larock, S. Iodine/palladium approaches to the synthesis of polyheterocyclic compounds. *J. Org. Chem.* **2010**, *75*, 1652–1658. [CrossRef] [PubMed]
43. Zhang, F.-B.; Adachi, Y.; Ooyama, Y.; Ohshita, J. Synthesis and properties of benzofuran-fused silole and germole derivatives: Reversible dimerization and crystal structures of monomers and dimers. *Organometallics* **2016**, *35*, 2327–2332. [CrossRef]
44. Frisch, M.J.; Trucks, G.W.; Schlegel, H.B.; Scuseria, G.E.; Robb, M.A.; Cheeseman, J.R.; Scalmani, G.; Barone, V.; Mennucci, B.; Petersson, G.A.; et al. *Gaussian 09, Revision D.01*; Gaussian, Inc.: Wallingford, CT, USA, 2013.
45. Farinola, G.M.; Ragni, R. Electroluminescent materials for white organic light emitting diodes. *Chem. Soc. Rev.* **2011**, *40*, 3467–3482. [CrossRef] [PubMed]